Construction and Building Materials 296 (2021) 123620

Contents lists available at ScienceDirect

Construction and Building Materials

journal homepage: www.elsevier.com/locate/conbuildmat

Compaction and volumetric analysis of cold in-place recycled asphalt mixtures prepared using gyratory, static, and impact procedures

P. Orosa *, A.R. Pasandín, I. Pérez

Universidade da Coruña, Department of Civil Engineering, E. T. S. I. Caminos, Canales y Puertos, Campus de Elviña s/n, 15071 A Coruña, Spain

HIGHLIGHTS

- CIR mixtures with 100% RAP were manufactured using 3 different compaction methods.
- The volumetric properties were obtained before and after curing by different methods.
- The volumetric results were compared with one another, and with the target and usual field values.
- The gyratory compaction was found to be the most suitable for CIR.
- Density by dimensions was useful for mix design; while the dry method best predicted field results.

ARTICLE INFO

Article history:
Received 5 February 2021
Received in revised form 23 April 2021
Accepted 10 May 2021

Keywords:
Cold in-place recycling/recycled (CIR)
Reclaimed asphalt pavement (RAP)
Asphalt mixture
Bitumen emulsion
Compaction
Gyratory compactor
Impact compaction
Marshall hammer
Static compaction
Bulk density
Volumetric properties

ABSTRACT

Compaction is one of the most important factors to be considered while manufacturing laboratory samples of cold in-place recycled (CIR) mixtures.

In this study, the effect of three laboratory compaction procedures (static, gyratory, and impact) on the volumetric performance of CIR mixtures was investigated. CIR specimens were manufactured with the same proportion of added water and bitumen emulsion, and using several levels of compaction, varying the number of gyrations and blows. The volumetric properties were evaluated by different procedures, both before and after curing. A comparison between the laboratory results of the different tests, the design target values, and actual in-field values was performed. It was observed that gyratory compaction proved to be the most versatile and one that best represented the real compaction. The bulk density procedure by dimensions was useful for laboratory design; however, it overestimated the sizes of the air void content by more than 10% compared to the field values.

1. Introduction

Cold in-place recycling (CIR) technology has started attracting increasing attention in maintenance and rehabilitation of stressed road pavements in recent years, as it is possibly one of the most cost-effective techniques and offers numerous advantages in terms of environmental sustainability and mechanical performance of the mixtures [1–3].

This rehabilitation process is aimed at obtaining reusable materials normally from worn-out pavements and using them in new mixtures for base or binder layers, as well as wearing courses. In this context, the most commonly used material is the reclaimed asphalt pavement (RAP). This process allows the use of a high amount of RAP as an aggregate. The easy availability of RAP implies a continuous supply of solid phase for the mixtures, while the use of virgin natural aggregates can be avoided, thus requiring less energy and transportation [4].

The main binder used in CIR is bitumen, which can be applied in the form of either bitumen emulsion or foam. Both of these bitumen materials allow a reduction in the viscosity of bitumen so that it can blend and compact these mixtures without heating. In this study, only the use of bitumen emulsion was considered, following the Spanish specifications for pavement recycling (known as PG-4) [5]. An additional amount of water is also normally added to the

* Corresponding author.
E-mail addresses: p.orosa@udc.es (P. Orosa), arodriguezpa@udc.es (A.R. Pasandín), iperez@udc.es (I. Pérez).

https://doi.org/10.1016/j.conbuildmat.2021.123620
0950-0618/

mixture, which reduces the internal friction among the particles and improves the workability and compactability of the mixture [6–8]. Additives, such as Portland cement and lime, are usually added to facilitate dispersion of bitumen in the cold mixture, regulate the breaking of the emulsion, accelerate the curing time, and improve the mechanical properties of the mixture [5,9]. In this study, CIR mixtures were manufactured with 100% RAP and with no additives.

In the context of the design of asphalt mixtures, it is a common practice to manufacture laboratory specimens and test them to predict the behaviour of asphalt pavements before their actual deployment in the field. Thus, to design high-quality pavements, it is essential to ensure the production of high-quality laboratory specimens for mechanical testing. One of the main steps in the manufacture of laboratory specimens is compaction, which involves a number of procedures and parameters.

Compared to field compaction, one of the advantages of compaction in the laboratory is that it allows a greater control of factors, such as the amount of energy used, material consumption, temperature, moisture, etc. [5,10,11]. Furthermore, it does not require the removal of the cores from an intact in-service road to test them. However, one of the main difficulties is the selection of the most appropriate compaction method and then setting its parameters such that the final specimens reproduce the mechanical and volumetric performance obtained in the field to the maximum extent possible.

Furthermore, it was also proven that even though laboratory compaction methods could produce laboratory samples with identical volumetric properties, different methods often result in asphalt mixtures with different mechanical properties. These differences in the mechanical behaviour are caused by the differences in the orientation of the particles and the general structure of the aggregates, which in turn, is because of the different methods of compaction and procedures used [10,11]. For this reason, numerous studies are being carried out to investigate the reasons for these differences among the existing laboratory compaction methods, as well as differences with in-field compaction, and their influence on the volumetric and mechanical properties [12,13].

Internationally, there are many compaction procedures for asphalt mixtures. Depending on the specific design methods used in each country, not only may the compaction procedures employed vary, but within the same method, some of the relevant parameters may also be applied in different magnitudes. This is the case for gyrations, internal rotation angle or speed in the gyratory compactor, pressure or time in the static procedure, number of blows in Marshall compaction, etc [11,13–15].

Particularly in Spain, in the design of a CIR mixture in a laboratory, the applicable standard is known as PG-4 [5,17]. The PG4 standard from 2001 [5] was updated in 2017 [17], and one of the main changes introduced was the required compaction method. Since 2017 the gyratory compactor has been recommended, while prior to that, the static compaction was used. Previous studies have already examined the differences between these two standards [18], and it was found that there were problems in achieving the mechanical requirements of the gyratory compacted mixtures with the current specification. Therefore, it was concluded that a revision and adjustment of this specification was needed.

While compacting CIR mixtures, a distinction must be made between the target density and the density achieved in practice. The target density is typically 97% to 100% of the dry density obtained in the laboratory using the modified proctor test (MPT), depending on the specification followed [5,15–17]. However, frequently, the densities reached in the field usually exceed these target values, based on the data obtained from the cores, owing to the type of compaction, traffic flow, and other factors.

Based on technical reports and scientific literature, it is possible to obtain an overall view of the volumetric behaviour of real CIR mixtures implemented on site [16]. Table 1 provides a framework for the field density documented in the literature, mainly resulting from density tests on extracted cores. It is important to point out that each particular study used a CIR mixture with a different RAP; in some cases, additives, different dosages of water and bitumen emulsion, and therefore the results were different.

As can be seen, in Table 1, the in-field densities for CIR mixtures are widely variable, ranging from 1879.80 to 2310.00 kg/m^3. The average in-field density from the explored literature was 2106.96 kg/m^3 for CIR mixtures.

2. Motivation

The lack of adequate knowledge on cold mixtures and their design makes it necessary to carry out more studies on CIR mixtures. There are many compaction studies of asphalt mixtures, which have aimed to adjust the existing compaction methods to achieve a compaction similar to that obtained in the field.

However, with regard to CIR mixtures, there has been no consensus and the results obtained have been very diverse. For example, the required number of turns of the gyratory compactor usually varies between 30 and 200 to reach the field reference densities according to different studies and reports [14,16,22,25–27]. These differences are sometimes because of the use of different additives or fillers in the mixtures (which facilitate compaction), or changes in certain parameters (e.g., internal rotation angle of the compactor) that significantly influence the volumetric properties obtained [14,28].

It was therefore decided to conduct a study with mixtures manufactured with 100% RAP, using different compacting methods, and varying their parameters to contribute further knowledge on this subject and gain a deeper understanding of the influence of different compaction procedures on the volumetric properties and final performance of the CIR mixtures. In addition, different standardised procedures were used to obtain such volumetric properties.

3. Aim and scope

This study was focused on the analysis of volumetric characteristics of CIR mixtures with bitumen emulsion. The main objective was to evaluate and compare the volumetric properties of CIR specimens manufactured using three of the most widely used laboratory compaction methods in Spain, namely gyratory, static, and impact (Marshall hammer), and by varying certain compaction parameters (e.g. compaction energy). To this end, considering the large volume of work involved in this study, it was divided into two parts.

In the first part, because of the great variability found in the literature in terms of gyrations used with the gyratory method, an in-

Table 1
Documented in-field density ranges for CIR mixtures.

In-field density range for CIR (kg/m^3)	Source
2120.84 – 2271.42	Diefenderfer et al. (2012) [19]
2026.00	Cox et al. (2015) [16]
2082.40	Lee et al. (2003) [20]
1948.00 – 2031.00	Sufian et al. (2008) [21]
1879.80 – 2105.80	Cross (2002) [22]
2040.00 – 2140.00	Martínez-Echevarría Romero (2012) [23]
2270.00 – 2310.00	Martínez (2007) [14]
2192.00	Miró (2007) [24]

depth study of this compaction method was conducted, using the complete range of gyration cases allowed by the compactor; while in the second part, samples were manufactured using the other two laboratory compaction methods (static and impact), following their respective standards. In both the cases, the main objective was to obtain the volumetric properties of the manufactured CIR specimens using these different procedures.

The CIR mixtures typically present higher voids content than traditional dense-graded HMA, so it was considered essential to use 3 different procedures to obtain the bulk density (geometrical, sealed specimen and dry procedures) and analyse the differences in the results.

Finally, the results were compared by analysing the compaction plots. This comparison allowed us to establish the equivalent compaction energy among the studied methods, define the most suitable laboratory compaction procedure to reach the target density, and reproduce the in-field behaviour as accurately as possible.

4. Materials and methods

4.1. Materials

4.1.1. Reclaimed asphalt pavement (RAP)

The studied CIR mixtures employed 100% RAP obtained by milling the superior part of worn out road asphalt pavements. The RAP was provided by a regional specialist contractor. Fig. 1 shows the size distribution of the used RAP, obtained following the Standard EN-12697-2 [29], and the gradation limits of the Spanish specifications for CIR mixtures [5].

The RAP had a bulk specific density of 2560 kg/m^3, which was obtained in accordance with EN 1097-6 [30]. The residual binder content, obtained according to the Spanish Standard NLT-164/90 [31], was 7.81% (by aggregate weight). Additionally, the recovered asphalt showed a ring and ball temperature of 64.4 °C, based on EN 1426 [32] and a penetration of 20.32 $\times$ 10^{-1} mm based on EN 1427 [33].

In comparison with other studies in the technical literature, the used RAP showed a coarse grain size. However, no grain size corrections were made to investigate what actually happens in a cold in-place recycling. Also, it is a RAP with a high binder content, which reflects the fact that it came from the milling of surface bearing layers, with higher concentrations of bitumen content than the other layers. The Spanish specification PG-4, followed for CIR [5], does not limit the use of RAP in this case; therefore, it was decided to use the same in this study.

4.1.2. Bitumen emulsion

The bitumen emulsion employed in this study was a C60B5 REC (according to EN 13808 [34] nomenclature). This implies a slow-setting cationic emulsion with 60% bitumen content (BC). The bitumen emulsion was supplied by a Spanish petroleum company. The ring and ball temperature, and the penetration values of the fresh residual bitumen used to produce the bitumen emulsion were 20.32 °C and 170.00 $\times$ 10^{-1} mm, according to EN 1426 [32] and EN 1427 [33], respectively.

4.1.3. Paraffin wax

The bulk density of the CIR specimens was calculated according to the standard EN 12607-6 [35], following procedure C, titled "Sealed specimen". As the CIR mixtures were very porous, paraffin wax was used to make the specimens waterproof by sealing them and preventing water from penetrating the accessible voids in the specimen. The density of the paraffin used was 800 kg/m^3, and its melting point was 56 °C.

4.2. Methods

4.2.1. Assessment of CIR compaction

As stated before, in view of the high volume of data in the compaction analysis conducted, it was decided to divide the study into two parts (Fig. 2):

- In the first part, an exhaustive study of the gyratory compaction method was conducted. The variation in the volumetric properties of the specimens was analysed depending on the variation in the number of gyrations performed during the compaction.
- In the second part, the specimens were manufactured using static and impact compaction, and the corresponding volumetric properties were also obtained.

Different procedures for obtaining the bulk density were performed to evaluate the differences. Finally, the obtained results were compared and a relationship among the methods studied was determined. In addition, the most appropriate compaction method for CIR and the best procedure to calculate the volumetric properties of the specimens were identified for meeting the design target density and the best estimation of in-field behaviour.

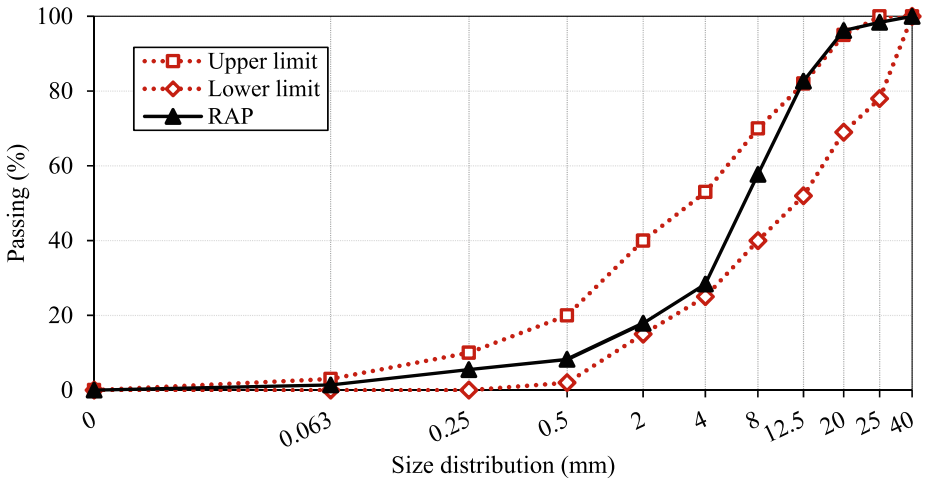

Fig. 1. RAP gradation compared with the limits from PG-4 specification.

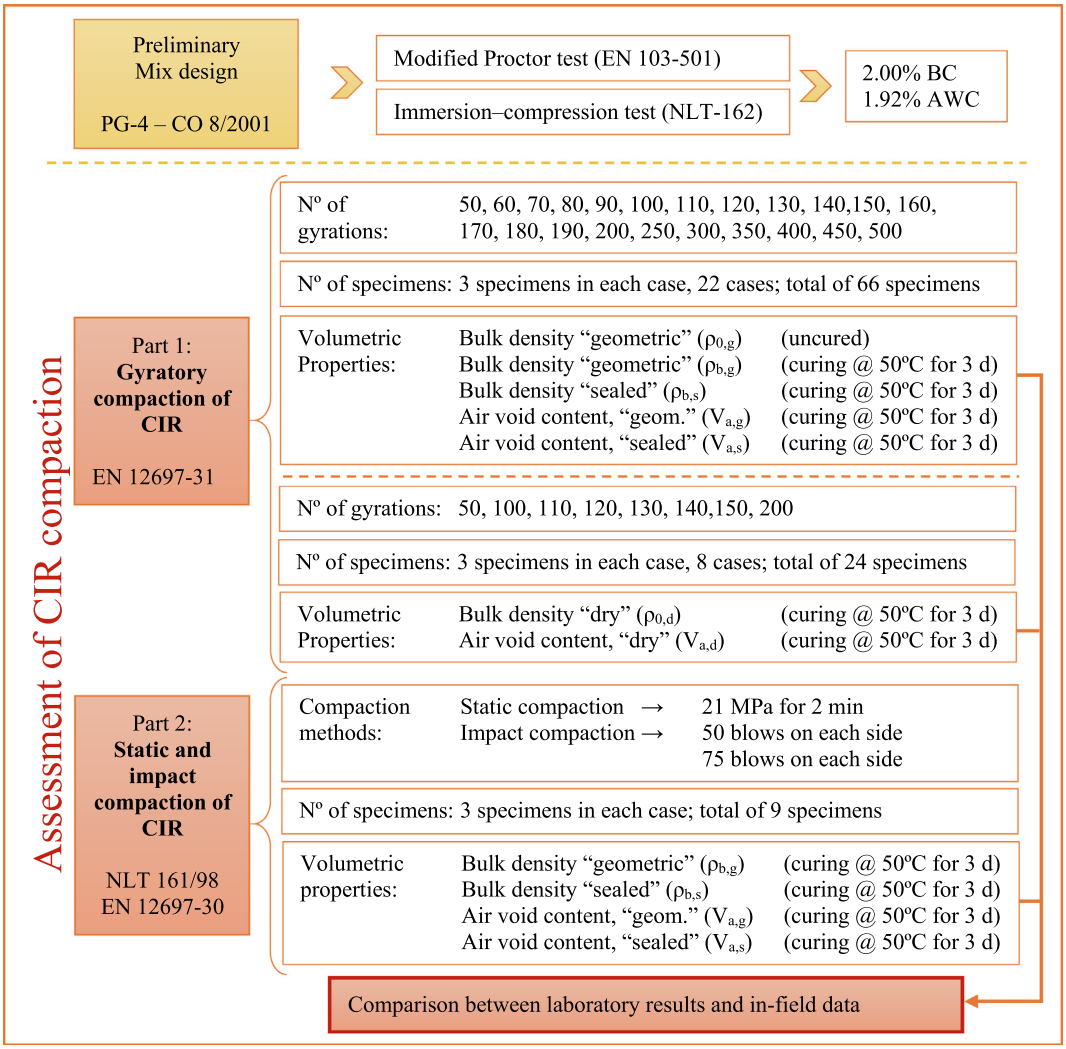

Fig. 2. Structural diagram of the study.

4.2.2. Preliminary work on mixture design

There is a multitude of design methods for CIR mixtures, both in the international scientific literature and in the related standards, and there is no universally accepted procedure. In this study, the design method described in the Spanish PG-4 specification for CIR mixtures was employed [5].

4.2.2.1. Modified Proctor test for added water content (AWC). Firstly, to obtain the optimum fluid content (OFC) of the studied CIR mixtures, modified Proctor tests were performed on the RAP following the EN 103–501 standard [36]. The RAP was placed in an oven for 24 h at 60 °C to completely dry the same and make the water content of the samples homogenous according to the specifications of PG-4 [5]. After returning the RAP to the ambient temperature (i.e. 20 °C), it was separated into six identical samples. The dry RAP samples were blended with various amounts of water, which ranged from 1.50% to 7.50%. The OFC representing the maximum dry density was determined by analysing the resulting dry density – water content plots. Finally, the AWC, which must be initially mixed with the RAP in the mixing process was obtained by Eq. (1) from PG-4 [5]:

$$AWC\ (\%) = OFC\ (\%) - 0.5 - EC\ (\%) \quad (1)$$

where AWC is the added water content; OFC is the optimum fluid content; and EC is the bitumen emulsion content that is added to the RAP (all values are percentages over the total RAP in the mixture).

4.2.2.2. Optimum binder content. According to the Spanish specification PG-4 [5], the job mix formula of the CIR mixtures needs to be validated by testing the sensitivity to water by means of the unconfined compression test (UCS). This test was performed following the Spanish Standard NLT-162 [37].

For this purpose, five series, each of which consisting of ten cylindrical specimens were manufactured and compacted using static compaction, by employing different residual BC and AWC. After the compaction, the specimens were cured at 50 °C in an oven for 3 d. Within each series, five specimens constituted the wet group and were conditioned by immersing them in water at 60 ± 1 °C, while five specimens constituted the dry group and were introduced into a climatic chamber at 25 ± 1 °C. The conditioning period was 1 d in all the cases, as stated in NLT-162. Just before the test was carried out, all the specimens were immersed in water at 25 ± 1 °C for 120 min.

The retained strength ratio (RSR) was calculated as follows:

$$\mathrm{RSR}(\%) = \frac{UCS_{wet}}{UCS_{dry}} \cdot 100 \quad (2)$$

where UCS_{wet} is the average of the unconfined compression strength of the samples in the wet group and UCS_{dry} is the average of the

unconfined compression strength of the samples in the dry group. Finally, the results obtained were compared, and the best percentage was selected, which met the minimum requirements of strength for the potential traffic categories.

4.2.3. Manufacturing of specimens

4.2.3.1. Mixing process. The mixing process was divided into two steps, which was followed for all the studied samples. To begin with, the RAP and added water were first mixed for 60 s; then the bitumen emulsion was added to the mixture; and they were mixed for an additional 90 s, which meant a total mixing time of 150 s. This mixing time was selected based on the previous results and studies [18,25], to ensure an adequate coating of the RAP, while still not breaking the bitumen emulsion.

To make the specimens as similar and the results as comparable as possible, all the specimens were produced with the same RAP content, and same water and bitumen emulsion proportions

4.2.3.2. Compaction methods. Once the mixing process was complete, the mixture was introduced into moulds for compaction. In this study, three different types of compaction were employed, namely gyratory, static, and impact procedures, which are described as follows.

a) Gyratory compaction

Gyratory compaction was conducted according to EN 12697-31 [38]. The dimensions of the specimens included a diameter of 99.7 mm and a height of 63.5 ± 1.5 mm, as these dimensions are considered to be suitable for volumetric studies; furthermore, these dimensions are widely used in different mechanical tests, for example, in the indirect tensile strength measurement. The gyratory specimens were produced using 950 g of RAP.

The parameters of the gyratory compactor (Fig. 3) included an internal angle of rotation of 0.82°, speed of 30 rpm, and compaction pressure of 600 kPa, as stated in the European standard EN 12697-31 [38]; these parameters remained constant throughout this study.

Fig. 3 shows all the steps followed during the gyratory compaction procedure, from the mixing of the sample (Fig. 3a) and its placement in the mould and in the compactor (Fig. 3b, 3c, and 3d), to the selection of compaction parameters (Fig. 3e), and final extraction of the specimen (Fig. 3f). Specimens compacted with the gyratory compactor were sufficiently stable to allow extrusion immediately and were stored for accelerated curing.

As there is no international consensus concerning the number of gyrations required to compact the CIR mixtures with this type of compactor, it was decided to carry out this study to assess this parameter's influence on the volumetric properties.

The highest number of gyrations allowed by the employed compactor was 500. Thus, as shown in Fig. 2, the specimens were compacted using 50, 60, 70, 80, 90, 100, 110, 120, 130, 140, 150, 160, 170, 180, 190, 200, 250, 300, 350, 400, 450, and 500 gyrations (as the range between 50 and 200 is the most frequently used), covering all the 22 groups, with each group comprising three specimens (a total of 66 specimens). These specimen groups were named with the prefix "G" followed by the number of gyrations used (e.g., G-50 for the group compacted with 50 gyrations, etc.). Another set of 24 specimens were manufactured to evaluate the volumetric properties following a different procedure. In this case, eight groups, with three specimens in each, were tested (with 50, 100, 110, 120, 130, 140, 150, and 200 gyrations), in the typically followed range of the number of design gyrations.

During the manufacturing process and after the curing procedure, several measurements of the specimen characteristics were recorded (diameters, heights, and weights) at different stages to effectively track the quality of the procedures. This verification was done in the following two ways:

By registering the weights of the specimens at different times: W1 represents the weights of the samples before being introduced into the compactor; W2 represents the weights of the specimens recently compacted and extracted from the compactor; and W3, the weights of the specimens after 3 d of curing in the oven. Based on these weights, we could estimate the weight loss during compaction (Δ1) during the curing procedure (Δ2), and the total loss (Δ) using Eqs. (3) to (5), respectively, as follows:

$$\Delta 1 = W1 - W2 \quad (3)$$

$$\Delta 2 = W2 - W3 \quad (4)$$

$$\Delta = \Delta 1 + \Delta 2 \quad (5)$$

Δ1 primarily refers to the loss of water during compaction, as the mould has holes through which water could drain off; it also refers to a possible loss of material, which remains stuck in the mould or falls out during handling (this is considered insignificant). Δ2 is the loss of water by evaporation during the accelerated curing. The addition of both the above quantities (total loss Δ) means the total loss of mass (≈ loss of water), from mixing and compaction procedures, until the specimen is considered to have lost all the water.

To confirm that the manufacturing was carried out correctly, Δ must be similar to the theoretical value of water included in the samples. As all the gyratory specimens were identically prepared, this content was the same in all the cases. The theoretical water content in the samples corresponds to the sum of the AWC and water, included in the emulsion (i.e., 40% of EC). For the gyratory specimens manufactured using 950 g of RAP, the total theoretical water content was 30.88 g.

Based on the difference between the geometric densities before and after the curing ($\rho_{0,g}$ and $\rho_{b,g}$, respectively), and assuming that the volume of the specimens (V) remained approximately constant. From this difference (Eq. (6)), it is possible to estimate the difference in the weight through Eq. (7), which is mainly owing to water evaporation (Δwater), which should be similar to the loss of water Δ2 obtained above.

$$\Delta\rho = \rho_{0,g} - \rho_{b,g} \quad (6)$$

$$\Delta water = \Delta\rho \cdot V \quad (7)$$

b) Static compaction

In accordance with NLT-161 [39], three CIR specimens with a diameter of 101.6 and a height of 100 mm were compacted by applying static compaction. A total of 1800 g of RAP was used to manufacture each specimen. This group of specimens compacted with the static press was designated with the prefix "S".

Fig. 4 shows the steps of this compaction method. It can be seen how, after mixing (Fig. 4a), the sample was placed into the corresponding mould with the help of a pike (Fig. 4b and c); subsequently, it was positioned in the machine for compaction (Fig. 4d–f). This compaction procedure consists of a one-min vertical preload of 1 MPa, followed by a two-min stage, during which the load was increased to 21 MPa linearly. This load was held for 2 min before being linearly reduced back to 0 MPa.

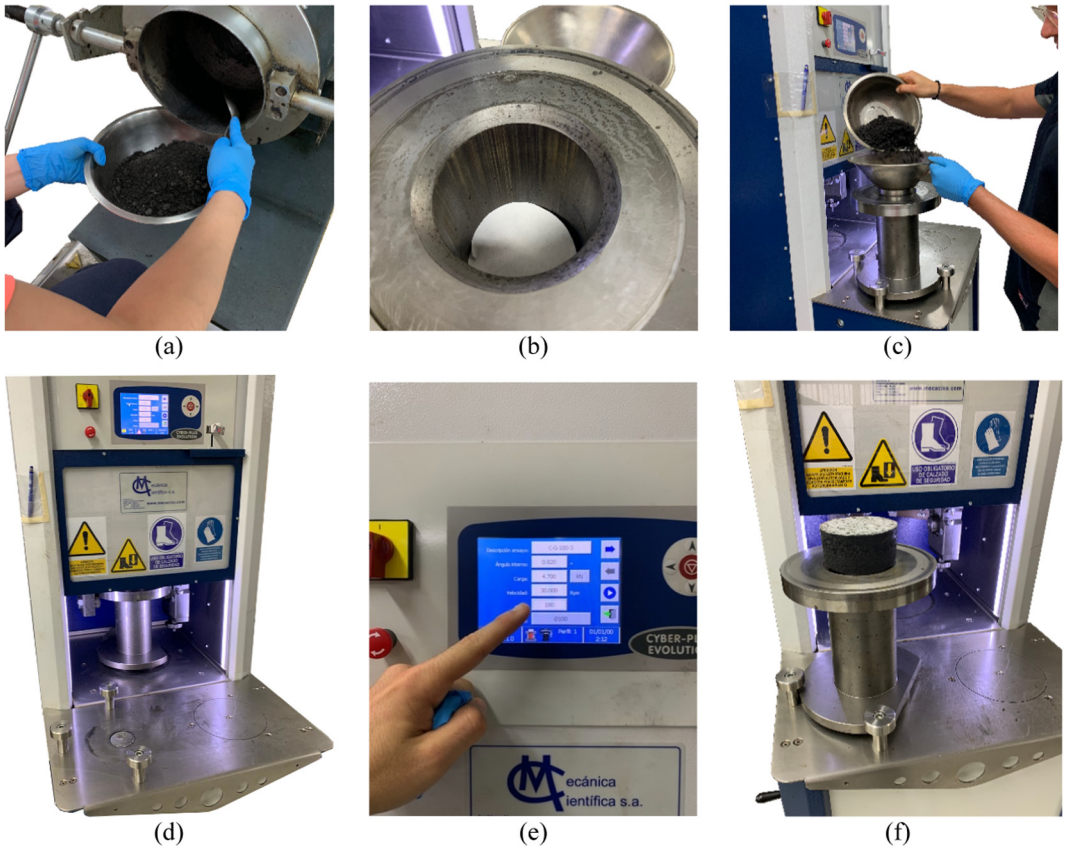

Fig. 3. Gyratory compaction procedure: (a) Sample mixing; (b) Mould preparation; (c) Sample placement; (d) Mould placement; (e) Parameter selection; (f) Extrusion of compacted specimen.

c) Impact compaction (Marshall hammer)

According to EN 12697–30 [40], two groups of three CIR specimens each, with a diameter of 101.6 mm and a height of 63.5 ± 1. 5 mm, were compacted using a Marshall hammer, and applying two different compaction energies. The first group was compacted with 50 blows applied on each side, while the second group was subjected to 75 blows. These groups of specimens were called M−50 and M−75, respectively. A total of 950 g of RAP was used in the manufacture of each specimen.

Fig. 5 shows the steps followed to perform the impact compaction. It starts with the mixing of the sample (Fig. 5a) and its placement in the corresponding mould with the help of a pike (Fig. 5b and c), and the placement of the mould and the hammer (Fig. 5d and e), to proceed with the Marshall compaction. Finally, Fig. 5f shows the collection of the weight of the compacted specimen.

4.2.3.3. Accelerated curing procedure. A curing time was necessary for the specimens before their volumetric properties were measured. Thus, immediately after each compaction, all the specimens were cured after being unmoulded for 3 d at 50 °C, following the PG-4 specifications [5]; this is the time required to reach a constant mass and thereby lose the existing water by evaporation.

4.2.4. Volumetric characterisation

Once all the specimens were cured, they were allowed to cool to the ambient temperature and their volumetric properties were obtained following different procedures (bulk density as well as the related air void content by dimensions method and sealed specimen method). Additionally, in the case of the group of gyratory specimens (G), the density values were also calculated before the curing procedure, soon after when they were extracted from the compactor. Furthermore, the bulk density of gyratory specimens was also measured by the dry procedure on cured specimens, for a more specific range of gyrations. Thus, the properties that were determined in this study are explained below.

- Maximum specific density, ρ_m

ρ_m represents the maximum specific density (kg/m^3), which was determined according to EN 12697-5 [41]; it was measured in loose mixtures with a pycnometer. The maximum density is an intrinsic material property related to the constituent materials and mixture composition; in this study, it was obtained as an average of three CIR samples.

- Initial geometric density, $\rho_{0,g}$ (data from gyratory compactor)

This density was calculated for the specimens compacted with a gyratory compactor, prior to the curing procedure. The Gyratory compactor was equipped with LDVT displacement transducers that record the evolution of the height (h) of the specimens with the number of cycles, during the compaction. For each sample, the weight was known prior to the compaction (W1) and was introduced as a parameter in the compactor. The compactor software would calculate the density in each cycle, assuming that the specimen diameter was equal to the inner diameter of the mould (100 mm), employing Eq. (8). This would allow the tracing of the compaction curve with the evolution of the density. Thus, the value of $\rho_{0,g}$ was adopted as the density value obtained in the last compaction cycle.

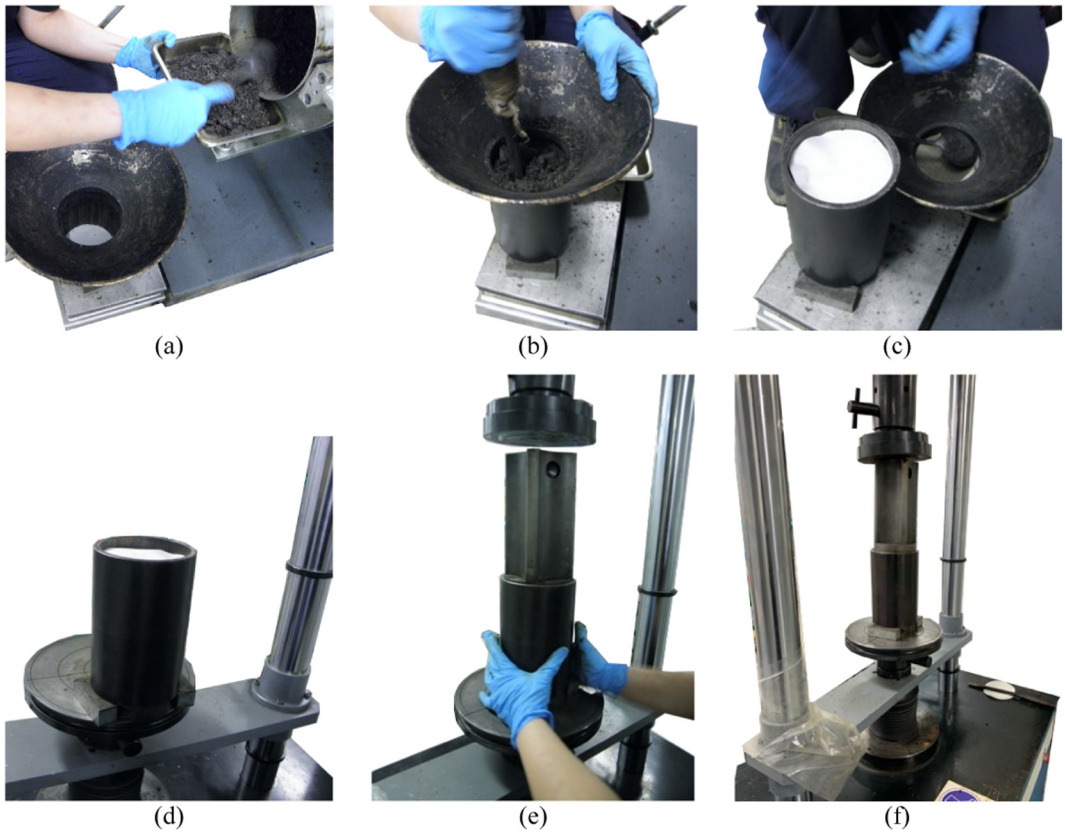

Fig. 4. Static compaction procedure: (a) Sample mixing; (b) Sample placement; (c) Sample placement II; (d) Mould placement; (e) Plunger placement; (f) Static press ready to compact.

Fig. 5. Impact compaction procedure: (a) Sample mixing; (b) Sample placement; (c) Sample placement II; (d) Mould placement; (e) Hammer placement; (f) Compacted specimen weighing.

Given the calculation procedure used by the compactor to obtain $\rho_{0,g}$, a potential correction was considered. Because the original calculation uses the diameter of the mould (constant), it was proposed to calculate a corrected $\rho_{0,g}$', using the real-measured diameters of the specimens (Ø), and verify the error accrued.

$$\rho_{0,g} = \frac{4 \cdot W1}{\pi \cdot 100^2 \cdot h} \quad (8)$$

$$\rho'_{0,g} = \frac{4 \cdot W1}{\pi \cdot Ø^2 \cdot h} \quad (9)$$

- Bulk density – Sealed specimen method, $\rho_{b,s}$ (*procedure C*)

After the specimens were cured, tempered, properly weighed, and measured, the bulk density $\rho_{b,s}$ was calculated by the "sealed specimen" method by applying procedure C described in EN 12697–6 [35]. For open asphalt mixtures, such as CIR (i.e. air void content of 10% or more), the paraffin-coated method is recommended. Paraffin makes the specimens waterproof and prevents water from entering the accessible pores of the specimens. However, it is important to apply the paraffin correctly [35] to prevent it from penetrating into the internal cavities of the test tube.

Fig. 6, presents various steps involved in the procedure for the calculation of $\rho_{b,s}$. It was necessary to cover the specimens with preheated wax to ensure that they were in a fluid state (Fig. 6a). Once the specimens were completely covered (Fig. 6b) and cooled to the ambient temperature (Fig. 6c), they were weighed dry and immersed in water (Fig. 6d), as indicated in the followed methodology [35].

- Bulk density by dimensions method, $\rho_{b,g}$ (*procedure D*)

After the accelerated curing process, when the specimens were at the ambient temperature, they were weighed and measured using a calliper (four heights and six diameters), according to procedure D described in EN 12697–6 [35]. The registered data allowed us to obtain the apparent density by "dimensions procedure" $\rho_{b,g}$, for each of the specimens in the study. This procedure is suitable for regular specimens (as is the case here), regardless of the level of voids in the specimen.

- Bulk density – dry, $\rho_{b,d}$ (*procedure A*)

This bulk density procedure was performed for another eight groups of specimens compacted with a gyratory compactor and cured within a specific range of gyrations, as the specimens used in the sealed specimen procedure could not be used for any further analysis.

EN 12697-8 [42], used for the estimation of air void content recommends to use this bulk density method (dry) in mixtures containing water.

To this end, the specimens were weighed after the accelerated curing process, once they were at the ambient temperature (mass of dry specimens). Next, the specimens were immersed in a water bath kept at a known temperature. The mass of the specimens was determined once they were stabilised. Using this information and following the Procedure A described in EN 12697-6 [35], the "bulk density – dry", $\rho_{b,d}$, was determined.

- V_a: Air void content

The percentage of air voids in the mixture was calculated following the standard EN 12697-8 [42], using the following equation:

$$V_a(\%) = \frac{\rho_m - \rho_b}{\rho_m} \cdot 100 \quad (10)$$

where V_a denotes the air void content (%); ρ_m is the maximum specific density (kg/m^3); and ρ_b is the bulk specific density (kg/m^3). As described above, the maximum specific density was calculated following the standard EN 12697–5 [41] and the bulk density was calculated according to EN 12697–6 [35], using procedures A, C, and D. Thus, the air void content was obtained for each of the previously calculated bulk densities. To differentiate among the three air void content results, they were named $V_{a,s}$, $V_{a,g}$, and $V_{a,d}$, depending on whether they were calculated from $\rho_{b,s}$, $\rho_{b,g}$, or $\rho_{b,d}$, respectively.

5. Results and discussion

5.1. Preliminary work on mixture design

5.1.1. Modified Proctor test for AWC

The modified Proctor test results revealed a maximum dry density of 1944.00 kg/m^3 for an OFC of 5.75% (Fig. 7). Hence, this is the OFC percentage used to calculate the AWC, in accordance with Eq. (1).

5.1.2. Optimum binder content

The bitumen content (BC) used in the manufacturing process of the CIR specimens was selected from the results of the immersion–compression test, described in NLT-162 [37], and in accordance with the requirements of the Spanish specification PG-4 [5].

Table 2 summarises the values of UCS_{dry} and UCS_{wet} obtained according to NLT-161 [39], and the RSR obtained for the different mix series tested by employing different BCs and AWCs, as well as the minimum requirements indicated in the PG-4 specification. In addition, the emulsion content (EC) was also indicated.

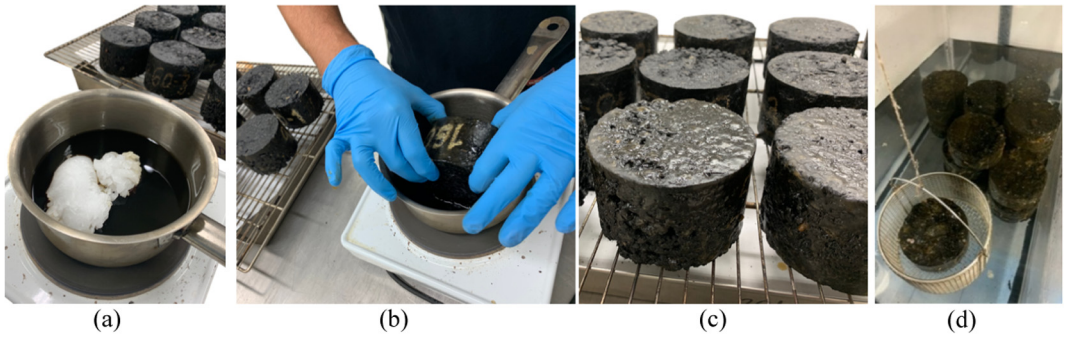

Fig. 6. Bulk density by sealed specimen procedure: (a) Paraffin wax melting; (b) Paraffin-coating procedure; (c) Paraffin-coated specimens; (d) Immersed specimen weighing.

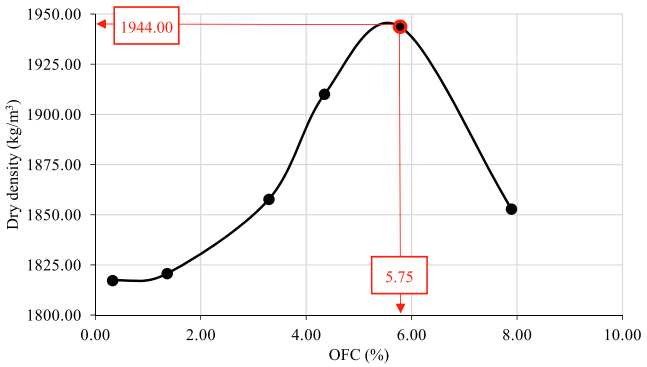

Fig. 7. Modified Proctor test results.

From Table 2, it can be seen that the RSR was higher than the lower limits of PG-4 specifications for all traffic categories. However, the UCS_{dry} and UCS_{wet} results satisfied the requirements only for lower traffic categories, T3, T4, and shoulders. This compliance was achieved for mix series 1, 3, and 4. For this reason, and in view of the best combination of the UCS and RSR, mix series 3 was selected. This job formula (BC of 2.00%, EC of 3.33%, and AWC of 1.92%) was employed for all the specimens studied in this research.

5.2. Assessment of CIR compaction

The results obtained from the volumetric analysis of the CIR mixtures using different compaction methods are shown in the following sections. As explained above, the study was divided into two parts, starting with an extensive analysis of the gyratory compaction method, varying the number of gyrations, and ending with the employment of static and impact compaction methods to compare and contrast the results obtained (Fig. 2).

To begin with, the calculation of the maximum specific density of the studied mixture (ρ_m) in accordance with EN 12697-5 [41] resulted in a value of 2419.22 kg/m^3.

As for the bulk density results of the manufactured specimens, it was decided to include in the comparison plots, a range of real in-field densities for this type of mixtures, obtained from technical literature, as well as the target density value specified in the followed Spanish guidelines for the design of CIR [5]. In this regard, as stated in Section 1, the in-field reference density for CIR (Table 1) ranged from 1879.80 to 2310.00 kg/m^3. The Spanish specification [5] indicates that the target density to be achieved in the field should be at least 100% of the maximum dry density obtained in the modified Proctor test. Thus, the target density considered for this particular studied mixture was 1944 kg/m^3 (Fig. 7).

5.2.1. Gyratory compaction of CIR

To carry out this study, 66 specimens were initially compacted using the gyratory compactor, varying the number of gyrations, first from 50 to 200, in steps of 10, and next from 200 to 500, in steps of 50. A total of 22 different gyration cases (i.e. specimen groups) were formed, each of which comprised three specimens. From these 66 specimens, the bulk density and air void content were determined using the procedures by dimensions and sealed specimens. Finally, another 24 specimens were manufactured to calculate these same volumetric properties by the dry method. In this second step, the gyrations used were 50, from 100 to 150 in steps of 10, and 200.

5.2.1.1. Bulk density and number of gyrations. The densities of the gyratory compacted specimens were calculated using four different procedures. Immediately after the compaction and without any curing time, $\rho_{0,g}$ was obtained directly from the compactor data. Once the accelerated curing period of 3 d at 50 °C was completed and the specimens were returned to the ambient temperature, ρ_b and V_a were also calculated by employing the three described methods ($\rho_{b,g}$ by the dimensions method, $\rho_{b,s}$ by the sealed specimen method, and $\rho_{b,d}$ by the dry method). These different bulk density results, as well as the above-mentioned reference range of in-field density and target value, are plotted together in Fig. 8. The markers on the density curves indicate the average result of the three specimens manufactured for each of the gyration cases, and the horizontal lines represent the in-field range and target densities. These three bulk density results after curing ($\rho_{b,g}$, $\rho_{b,s}$, and $\rho_{b,d}$) for each gyration case are also shown in Table 3.

It can be seen from Fig. 8 that $\rho_{0,g}$, which was calculated prior to the curing period, was higher than that obtained after the curing, using the procedures by dimensions and sealed specimen. This result was expected as the space filled by water was replaced by air after curing, and therefore the density would decrease in proportion to this water loss.

Related to this water loss, another outstanding feature of the results shown in Fig. 8 is the shape of the two geometric density curves, $\rho_{0,g}$ and $\rho_{b,g}$, both of which were calculated simply from the dimensions and weight of the specimens. Both geometric density curves have a similar shape, with a practically constant offset. This offset represents a decrease of 2.20% in the density, mainly owing to the aforementioned loss of water during the curing procedure. The similarity in shape also reveals that the calculations were performed correctly, as the loss of water (and proportional drop in density) was similar in all the gyratory specimen groups.

The bulk densities calculated by the sealed specimen and dimensions procedures (i.e. $\rho_{b,s}$ and $\rho_{b,g}$) were very similar; however, there was a certain tendency for $\rho_{b,s}$ to be higher than $\rho_{b,g}$. This difference represents an average increase of 1.50% for $\rho_{b,s}$ with respect to $\rho_{b,g}$. This difference was particularly relevant in the compaction with less energy; this difference reaches 3.50% for 50 gyrations, and decreases with an increase in the gyrations to only 0.65% for 500-gyrations case.

As previously mentioned, considering the proper procedures followed in each case, a slight overestimation of $\rho_{b,s}$, and an under-

Table 2
Results of the Immersion–compression test and PG-4 requirements.

	Specification limits*		Mix Series				
	T1 (base) and T2	T3, T4, and shoulders	1	2	3	4	5
BC (%)			1.50	1.75	2.00	2.25	2.50
EC (%)			2.50	2.92	3.33	3.75	4.17
AWC (%)			2.75	2.33	1.92	1.50	1.08
UCS_{dry} (MPa)	3.00	2.50	2.71	2.21	2.61	2.60	2.29
UCS_{wet} (MPa)	2.50	2.00	2.25	1.95	2.30	2.25	2.04
RSR (%)	75.00	70.00	83.34	88.41	88.25	88.56	88.88

*Traffic category T1: 2000 > Annual average daily heavy traffic (AADHT) ≥ 800; Traffic category T2: 800 > AADHT ≥ 200; Traffic category T3: 200 > AADHT ≥ 50; Traffic category T4: AADHT less than 50

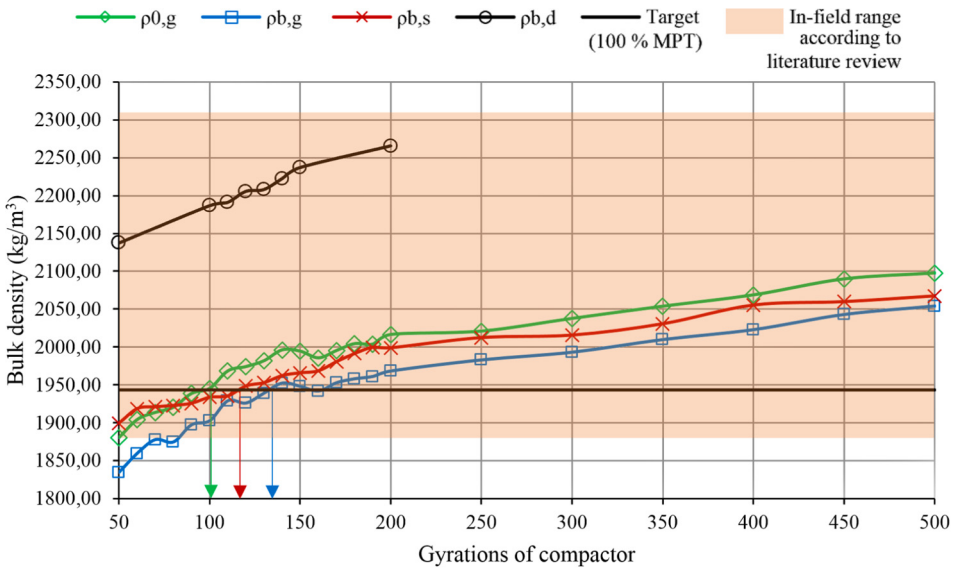

Fig. 8. Bulk density results of gyratory compacted specimens.

Table 3
Bulk density of gyratory specimens and water loss estimation during manufacturing and curing procedures.

	$\rho_{b,g}$ (kg/m^3)	$\rho_{b,s}$ (kg/m^3)	$\rho_{b,d}$ (kg/m3)	W1 (g)	W2 (g)	W3 (g)	Δ1 (g)	Δ2 (g)	Δ (g)
G-50	1834.68	1899.63	2137.52	996.87	993.33	962.67	3.53	30.67	34.20
G-60	1859.59	1918.81		997.10	993.87	963.43	3.23	30.43	33.67
G-70	1877.69	1921.19		997.33	994.63	966.07	2.70	28.57	31.27
G-80	1874.62	1922.93		997.23	993.70	963.83	3.53	29.87	33.40
G-90	1897.45	1925.82		997.20	994.13	965.23	3.07	28.90	31.97
G-100	1902.69	1933.74	2186.79	997.17	993.43	966.97	3.73	26.47	30.20
G-110	1929.10	1935.44	2191.16	997.27	994.00	967.00	3.27	27.00	30.27
G-120	1926.06	1948.62	2205.61	997.27	993.97	966.77	3.30	27.20	30.50
G-130	1939.22	1952.94	2208.06	997.27	993.77	967.17	3.50	26.60	30.10
G-140	1952.35	1962.30	2222.39	997.23	993.87	967.00	3.37	26.87	30.23
G-150	1948.06	1965.89	2236.96	997.27	993.90	967.40	3.37	26.50	29.87
G-160	1941.93	1968.59		997.33	993.63	965.03	3.70	28.60	32.30
G-170	1952.86	1980.79		997.30	993.77	964.17	3.53	29.60	33.13
G-180	1958.05	1991.50		997.27	993.87	964.67	3.40	29.20	32.60
G-190	1961.08	1999.79		997.27	993.83	964.50	3.43	29.33	32.77
G-200	1968.32	1999.09	2265.40	997.23	993.47	966.47	3.77	27.00	30.77
G-250	1982.99	2012.46		996.70	993.70	966.60	3.00	27.10	30.10
G-300	1993.18	2015.76		996.93	993.97	966.90	2.97	27.07	30.03
G-350	2009.90	2030.71		997.07	994.20	967.37	2.87	26.83	29.70
G-400	2022.96	2055.34		996.20	992.90	966.47	3.30	26.43	29.73
G-450	2042.96	2059.81		996.17	992.87	966.43	3.30	26.43	29.73
G-500	2054.11	2067.39		995.53	992.70	966.37	2.83	26.33	29.17
Average				997.01	993.70	965.84	3.30	27.86	31.17

estimation of $\rho_{b,g}$ was common. Regarding the sealed specimen procedure, part of the paraffin could penetrate the internal pores, increasing the density. In the case of the dimensions method, because the surface pores were counted together with the internal pores, there was a tendency to obtain lower densities. Therefore, the trend of the density results obtained using these two procedures was considered logical. However, although for this type of mixture with a high volume of air voids, it is recommended to use the sealed specimen method, the differences were minimal.

The bulk density by dry procedure (i.e. $\rho_{b,d}$) was also calculated, as it is recommended for estimating the volumetric properties of mixtures containing water [42]. This method was only performed near the range of gyrations recommended by the current PG-4 specification [17]. Because CIR mixtures are very porous, and the dry procedure uses the weight of the immersed specimens (and water penetrates the pores), $\rho_{b,d}$ values were significantly higher than those obtained with the other two methods (Fig. 8); it was, on average, 13.18% higher than $\rho_{b,s}$ and on an average, 14.31% higher than $\rho_{b,g}$, for the corresponding gyration cases.

It is also interesting to analyse the in-field reference range and target densities, as shown in Fig. 8, by comparing them with the densities obtained for different numbers of gyrations. It is worthwhile and sensible to compare with the results obtained after the curing period (i.e. $\rho_{b,g}$, $\rho_{b,s}$ and $\rho_{b,d}$), as these would be the reference values once the water content in the mixture was evaporated. Regarding the value of the considered target density, this value of $\rho_{b,g}$ was reached after 140 gyrations, and after 120 gyrations in the case of $\rho_{b,s}$ (Table 3). It should be noted that, without being initially the objective, it has been found that the range of compaction turns was rather consistent with the Spanish specification from 2017, described in Circular Order 40/2017 [17], which recommended using between 100 and 160 gyrations, depending on the granulometry of the RAP, and diameter of the moulds. $\rho_{b,d}$ was also obtained near the range, in which the values of $\rho_{b,s}$ and $\rho_{b,g}$ reached the tar-

get density. As already mentioned, $\rho_{b,d}$ was much higher than $\rho_{b,s}$ and $\rho_{b,g}$; it was also higher than the density target proposed by the Spanish PG-4 specification.

Regarding the range of in-field densities considered for the CIR, in practically all the cases, the results obtained could be framed within the range for all the apparent density procedures evaluated. In the case of $\rho_{b,d}$, the results were closer to the middle of the range, at the lowest number of gyrations, whereas for $\rho_{b,s}$ and $\rho_{b,g}$ an unusually high number of gyrations were necessary to reach the middle values of the CIR in-field density range.

As is already known, the variability of the CIR mixtures is high. According to the technical literature consulted, the range of compaction gyrations used to reach field densities is usually between 30 and 200 cycles [14,16,22,25–27], as was the case for $\rho_{b,d}$ (Fig. 8). This difference in the CIR compaction could be mainly owing to factors related to the materials used (the granulometry of the RAP, use of stabilisation additives, such as Portland cement or hydrated lime, or proportions of EC and AWC) as well as other factors related to the proper compactor parameters, such as the internal rotation angle.

Raschia et al. [7] highlighted the important effect of aggregate particle size on the properties of cold recycled mixtures. Adequate granulometry, together with the use of recycling additives, strongly facilitates the compaction of mixtures [25]. For this study, the coarse fraction of the RAP was high and no additives or fillers were used, which would explain the major difficulty in achieving higher bulk densities. Thus, in the case of $\rho_{b,s}$ and $\rho_{b,g}$, needing a higher number of gyrations to reach comparable density to in-field data was an expected result.

The AWC is also a relevant parameter in view of the related scientific literature, in terms of not only the compatibility, but also the mechanical properties of the mixtures [27]. While the design method followed indicates that to achieve the optimum moisture content of the mixtures studied, the AWC should be 1.92%, the AWC used in other studies revealed that 3.00% to 4.00% was usually the amount of added water that gave the best results [18,25,26]. The AWC could aid in reducing the internal friction between the aggregates and therefore, an increase in this content could facilitate the compaction process. In this study, the fact that a higher number of gyrations was obtained indicates that the AWC may have been insufficient, and the formulation given in Eq. (1) requires to be revised.

Regarding the internal rotation angle of the gyratory compactor, Martínez et al. [14] concluded that this parameter significantly influenced the compaction, which reached significantly higher densities for the same number of gyrations when the angle of inclination was higher. In most of the compaction studies that involved gyratory studies, the angle used was 1.25°, while the Spanish EN 12697-31 [38] standard suggests that an angle of 0.82° be used. The use of this lower internal rotation angle also involved that lower densities were reached.

In addition, in view of the results, it can be concluded that for 120 to 140 gyrations, $\rho_{b,s}$ and $\rho_{b,g}$, respectively, reached the target density, and were in the range of in-field reference densities for this type of CIR mixtures (however, in the lower part of the range and for a high number of gyrations). It was confirmed that the range of gyrations proposed by the Spanish specification followed for the CIR design [17] was in accordance with the target density proposed, as confirmed by both dimensions and sealed specimen procedures. Regarding these two density methods, it can be concluded that the difference between the results was very small for the range of gyrations considered (less than 1.00%). Therefore, estimating the bulk density with the geometric procedure was considered sufficient for the design method, as it was simpler to perform and it also allowed the specimens to be reused for other tests.

Even though the values obtained by the dry procedure were much higher than the target proposed in the design method, they were closer to the average values of the usual range of in-field densities, even for the lowest gyrations case, which was expected from the literature.

5.2.1.2. Accuracy of results by weight difference. Regarding the losses during manufacturing and curing procedures, a relationship could be established between the weight variations and the commented loss of water. As mentioned above, in Section 4.2.3.2, such a relationship could be traced by measuring (i) the weights of the samples before they were introduced into the compactor (W1), (ii) the weights of the recently compacted samples (W2), and (iii) the weights of the samples after the 3-d curing in an oven (W3). By knowing these weights, it was possible to estimate the losses that occurred during the compaction ($\Delta 1$) and the curing procedure ($\Delta 2$) by using Eqs. (3) and (4). These losses mainly correspond to water evaporation and are shown in Table 3.

The results in Table 3 show that the average Δ (31.17 g) was practically identical to the theoretical water content of the samples (30.88 g), with a difference of only 0.94%. This fact allows us to conclude that the loss of weight during the manufacturing and curing processes corresponded mainly to the loss of water by evaporation, as already stated.

5.2.1.3. Correction of $\rho_{0,g}$ and accuracy of results by density difference. The gyratory compactor automatically estimated $\rho_{0,g}$, based on the measured data inserted by the user using Eq. (8). For each sample, the weight was inserted manually in the compactor software, and the diameter considered corresponded automatically with the inner diameter of the mould used (100 mm in this case). The compactor was equipped with LVDT displacement transducers that would allow the user to know the evolution of the height (h) of the specimen throughout the compaction. Thus, using these measures, it was possible to know the density by the geometric method, $\rho_{0,g}$, in each gyration, prior to the curing procedure.

By analysing the data used in the calculation of $\rho_{0,g}$, it could be seen that both the heights of the specimens and their masses were actual values that were directly measured, manually, or via LVDT. The weight was manually measured by weighing the sample before its placement in the mould, and the height was measured via the LVDT transducers. However, the diameter of the mould did not correspond completely to the actual diameters of the specimens. While the diameter used for the calculation of $\rho_{0,g}$ was the diameter of the mould (100 mm), the average of the real diameters of the specimens, manually measured after compaction, was 99.74 mm. This slight error of 0.30% in the value used for the diameter led to an average error of 0.50% in the case of $\rho_{0,g}$. Thus, it was decided to perform a "manual calculation" of the initial geometric density ($\rho_{0,g}$'), by using the average of the measured real diameters of the specimens (Ø) instead of the mould diameter. In Fig. 9, $\rho_{0,g}$, and $\rho_{0,g}$' are represented. Again, the curve markers indicate the average value of the three specimens in each case in Fig. 9. It also represents the Δwater and Δwater', and the loss of water $\Delta 2$ obtained above by the difference in the weights of the specimens (Table 3).

By knowing the geometric density before and after the curing ($\rho_{0,g}$ and $\rho_{b,g}$), and assuming that the volume of the specimens (V) remained constant after this process, it was possible to estimate the loss of water (Δwater) during curing using Eq. (7). Thus, based on the results shown in Table 3, Δwater should be similar to $\Delta 2$ (27.86 g), i.e., the average loss of water by evaporation during the curing process. By using $\rho_{0,g}$ for this estimation, the average Δwater was 21.93 g (Table 4), which was 21.28% lower than $\Delta 2$. If $\rho_{0,g'}$ was used for the estimation of Δwater instead of $\rho_{0,g}$, the result varied significantly. Because the value of $\rho_{0,g}$ was lower than

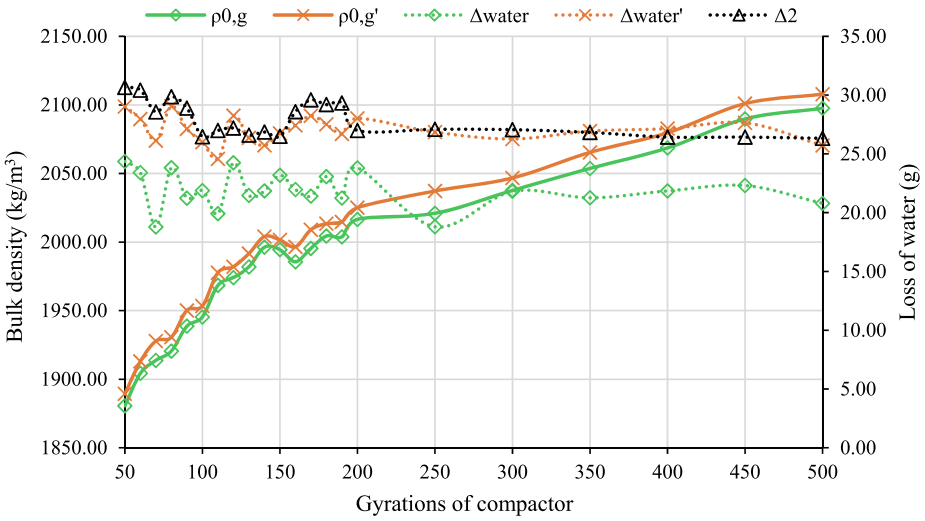

Fig. 9. Correction of $\rho_{0,g}$ in terms of the diameter and loss of water estimation.

Table 4
Initial geometric density calculated by compactor, corrected, and water loss estimation.

	$\rho_{0,g}$ (kg/m³)	$\rho'_{0,g}$ (kg/m³)	Ø (mm)	*h* (mm)	V (mm³)	Δρ (kg/m³)	Δρ' (kg/m³)	Δwater (g)	Δwater' (g)
G-50	1880.62	1889.43	99.77	67.50	5.30E + 05	45.94	54.75	24.36	29.03
G-60	1904.31	1913.01	99.77	66.66	5.24E + 05	44.72	53.42	23.41	27.97
G-70	1913.75	1927.86	99.63	66.33	5.21E + 05	36.05	50.16	18.78	26.13
G-80	1920.53	1930.60	99.74	66.10	5.19E + 05	45.91	55.98	23.83	29.06
G-90	1938.73	1950.20	99.71	65.48	5.14E + 05	41.28	52.75	21.23	27.13
G-100	1945.38	1953.40	99.79	65.26	5.13E + 05	42.69	50.71	21.88	25.99
G-110	1968.44	1977.66	99.77	64.45	5.06E + 05	39.34	48.56	19.91	24.58
G-120	1974.08	1982.00	99.80	64.31	5.05E + 05	48.02	55.94	24.25	28.25
G-130	1981.90	1991.62	99.76	64.05	5.03E + 05	42.68	52.41	21.47	26.36
G-140	1996.25	2004.04	99.81	63.39	4.98E + 05	43.90	51.68	21.85	25.73
G-150	1994.45	2001.56	99.82	63.65	5.00E + 05	46.39	53.50	23.19	26.75
G-160	1985.64	1996.49	99.73	64.00	5.03E + 05	43.71	54.56	21.97	27.43
G-170	1995.44	2009.04	99.66	64.03	5.03E + 05	42.58	56.17	21.41	28.25
G-180	2004.44	2013.38	99.78	63.33	4.97E + 05	46.39	55.32	23.07	27.52
G-190	2003.79	2014.74	99.73	63.35	4.98E + 05	42.71	53.67	21.25	26.70
G-200	2016.56	2025.10	99.79	62.86	4.94E + 05	48.23	56.78	23.81	28.03
G-250	2020.97	2037.23	99.60	63.03	4.95E + 05	37.98	54.25	18.80	26.86
G-300	2037.65	2046.74	99.78	62.47	4.91E + 05	44.47	53.56	21.82	26.28
G-350	2053.71	2065.39	99.72	61.81	4.85E + 05	43.81	55.50	21.27	26.94
G-400	2068.63	2079.71	99.73	60.94	4.79E + 05	45.67	56.75	21.86	27.16
G-450	2089.78	2100.97	99.73	60.69	4.77E + 05	46.82	58.01	22.31	27.65
G-500	2097.57	2107.86	99.76	60.94	4.79E + 05	43.46	53.75	20.80	25.73
Average			99.74			43.76	54.01	21.93	27.07

$\rho_{0,g}$', the value of Δwater' estimated this time was higher. The average Δwater' was 26.93 g (Table 4). This estimated value was closer to Δ2, differing only by 3.34%, thus resulting in a better approach of Δwater, with a gap of more than 5 g. Table 4 summarises the original initial geometric density as well as the corrected one; the real diameter, height, and volume of the compacted specimen; the difference between the geometric densities before and after curing (original and corrected); and the water loss values (original and corrected).

From this result, it was concluded that, in fact, the density registered in the compactor ($\rho_{0,g}$) was under-predicted owing to the use of the diameter of the moulds for the calculation, which was higher than the real one. However, despite this small calculation error, it was still a useful tool because it allowed us to track the compaction process, giving us the height and density curves throughout the process.

5.2.1.4. Air void content. Based on the relationship between the air void content and bulk density, the shapes of the air void content curves were analogous, but inverse, to those of the bulk density, as shown in Fig. 10. The curve markers in Fig. 10 indicate the average results of the air void content of the gyratory groups studied, obtained from the three bulk density results previously discussed.

It is not common to specify a range for the air void content in the recommendations for the CIR mixtures; therefore, no specific target value was available in the existing design methods. However, from the in-field results of recycled mixtures of this type, despite the high variability of the CIR, it was known that the air void content was usually around 8% – 16% [6,16,43,47]. This range was also represented in Fig. 10 by a shaded area.

As is well known and can be checked in Fig. 10, the air void content decreased with an increase in the binder content. According to the literature review and design recommendations, 2.50% to 4.00% of bitumen emulsion by weight of dry RAP was usually used in CIR mixtures. In this case, 3.30% of bitumen emulsion was used (2.00% of residual binder content).

Through an analysis of Fig. 10, it can be seen that the air void content estimated on the basis of bulk density from the sealed

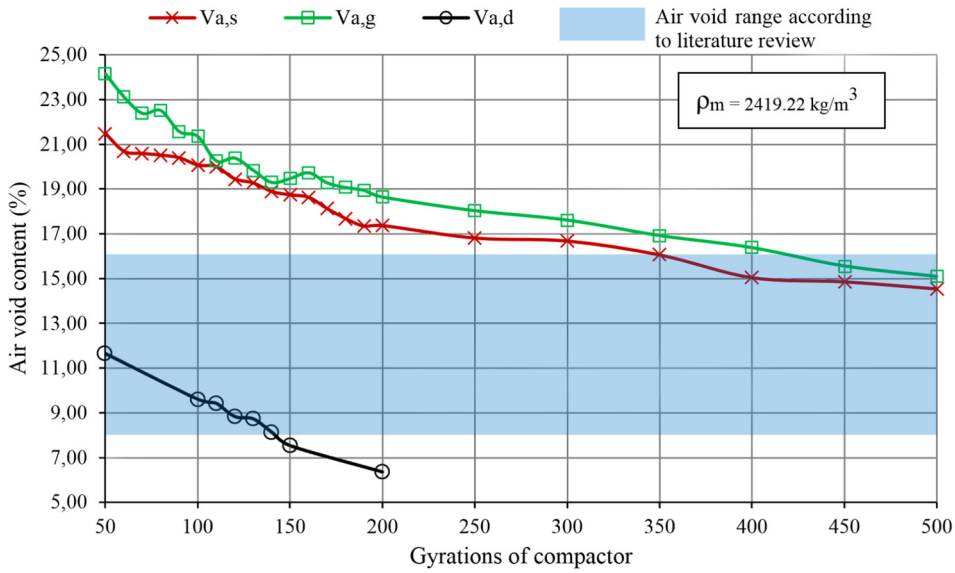

Fig. 10. Air void content of gyratory compacted mixtures after the curing period.

specimen and dimensions procedures (i.e. $V_{a,s}$ and $V_{a,g}$) were very high. To reach the usual in-field range of V_a, it would be necessary to compact the specimens using a large number of gyrations, ranging from 350 to 500 turns. In this case, for the usual number of gyrations, the volume of air voids was excessive, approximately 20%, which was more typical of a draining mixture.

However, for $V_{a,d}$, less than 12% of the air void content was already reached for 50 gyrations, which was in line with the in-field reports. The dry bulk density is the recommended procedure to obtain the volume of air voids in this type of mixtures [42]. From the results, it was confirmed that the bulk density by the dry procedure gave volumetric results (i.e., density and air voids) closer to those reported from the field than the other two considered procedures, which estimated 10% to 12% higher air void content.

5.2.2. Static and impact compaction of CIR

In the second part of the study, a group of three CIR specimens were compacted by using the static compaction (S), and another two groups of three CIR specimens each were compacted using the Marshall hammer, by applying 50 and 75 blows on each side (M−50 and M−75, respectively).

After the accelerated curing procedure of 3 d in an oven, $\rho_{b,s}$, and $\rho_{b,g}$ were obtained. For each of the bulk densities, $V_{a,s}$ and $V_{a,g}$ were also calculated using Eq. (10). In Fig. 11 the bars and markers indicate the average results obtained for groups S, M−50, and M−75. The in-field reference density range and target density values are also indicated.

In the case of specimens compacted with the impact method (i.e., M−50 and M−75), Fig. 11 shows that $\rho_{b,g}$ was lower than $\rho_{b,s}$. The difference was 4.15% in the case of M−50 and 3.28% in the case of M−75. These groups did not achieve the target density or even the lower limit of the range of in-field reference densities. Furthermore, as the density results achieved were the lowest, the air void content was excessively high, over 20% in all the cases, and even reached 25%.

As for the static compacted specimens (S), $\rho_{b,s}$ was 1.33% higher than $\rho_{b,g}$, confirming once again the similitude of the two procedures. In this case, the values of $\rho_{b,s}$ and $\rho_{b,g}$ achieved were much higher than the target density marked in the Spanish specification for CIR mixtures, on an average, by 13.08%. However, these results were still within the usual range of densities obtained at the worksite, and the average air void content of 8.53% – 9.75% was also an accepted range for the CIR according to field reports.

5.2.3. Comparison and discussion of results from compaction methods for CIR

In addition to analysing the volumetric results of the three studied compaction methods separately, the other main objective of this study was to compare them with one another and discus their trends. The bar chart of Fig. 12 shows the range of bulk densities obtained using the three studied compaction procedures. Only five groups of gyratory compacted specimens are represented in Fig. 12.

In summary, for the gyratory specimens (G), as seen and discussed above, the increase in the density with the number of compaction gyrations was as expected. As seen in Table 3, the target density was reached by $\rho_{b,s}$ after 120 gyrations, and by $\rho_{b,g}$ after 140 gyrations (within the range recommended by the current PG-4). As already mentioned, $\rho_{b,d}$ values were much higher than those of $\rho_{b,s}$ and $\rho_{b,g}$; furthermore, they were also higher than the target density for all gyrations. With respect to the reference in-field density range, almost all the results were within the range; however, it was concluded that $\rho_{b,d}$ and $V_{a,d}$ approximated the real volumetric behaviour better than the other procedures for gyratory compacted specimens.

By applying a static compaction with a load of 21 MPa, the specimens achieved the highest $\rho_{b,s}$ and $\rho_{b,g}$ in the entire study, even much higher than those obtained for 500 gyrations with gyratory compaction; this was 5.61% higher in the case of $\rho_{b,s}$, and up to 7.72% higher in the case of $\rho_{b,g}$. The average value of ρ_b achieved in the S group was 2198.02 kg/m^3. It was also found to be much higher than the considered target density. However, these results were comparable to those obtained for $\rho_{b,d}$ in the gyratory cases, which were considered to be a more accurate estimation of the in-field behaviour.

Despite obtaining volumetric results that may fit within the in-field density range derived from the literature review, the compressive system (static) was not considered to be the most accurate compaction method for CIR mixtures. The enhanced density is usually associated with increased loading pressure applied to the samples, which causes aggregate breakage and binder squeezing, as detected by other researchers [13,44,45]; which usually results in

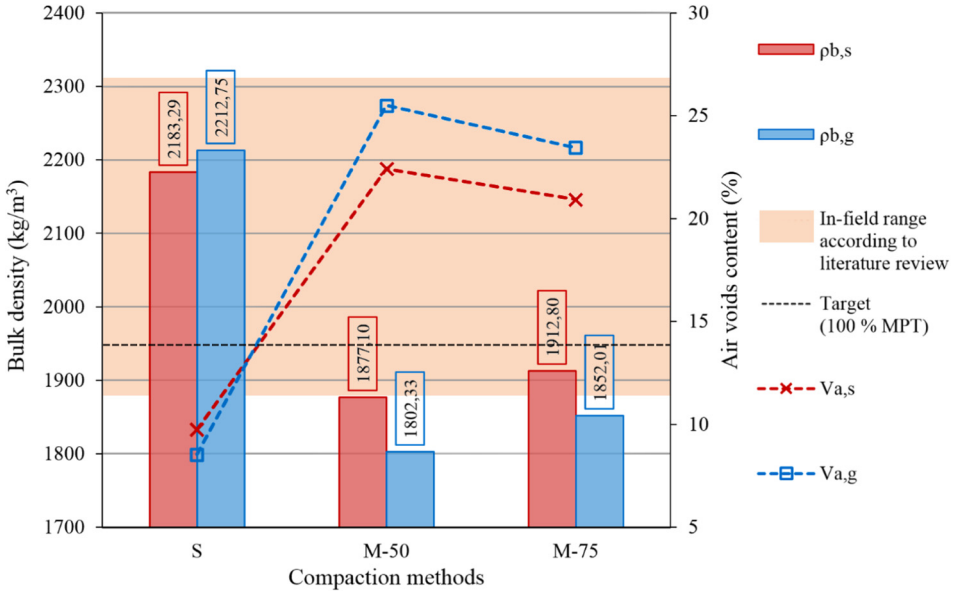

Fig. 11. Bulk density and air void content of mixtures compacted with static and impact procedures.

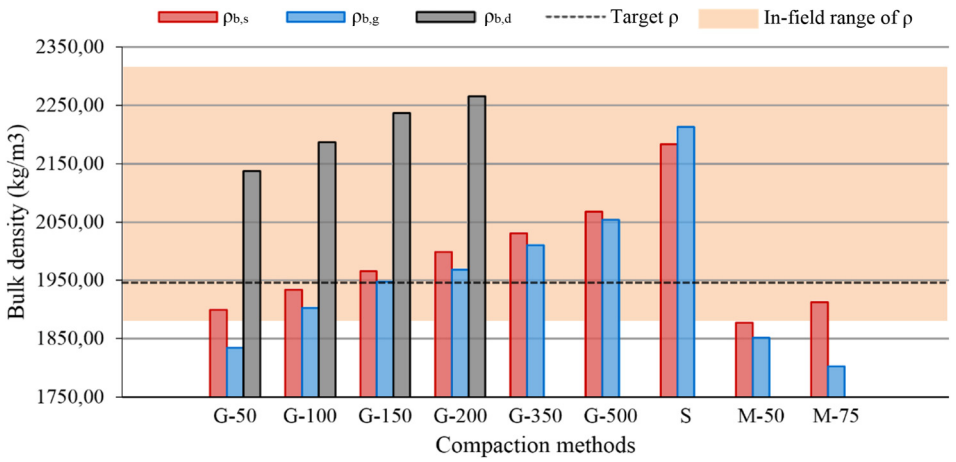

Fig. 12. Comparison of ρ_b from different compaction methods.

a much higher density in static compacted specimens than that obtained from in-field cores and other laboratory compaction methods. This tendency to obtain much higher density results with static compaction than with other methods has also been reported in other compaction studies [18,23,28,44]. Thus, this compaction method was not recommended for CIR mixtures.

Specimens from groups M−50 and M−75 did not reach the minimum target density. The average ρ_b of M−50 was 1839.71 kg/m^3, which was even lower than that obtained for G-50. The average ρ_b obtained for M−75 was 1882.40 kg/m^3, which was similar to that obtained for G-60 or G-70. Although the density of group M−75 was above the lower limit of the in-field density range, it was still considered a fairly low density value. For this reason, as already stated, impact compaction was not recommended in cold mixtures because it delivered worse volumetric characteristics than those obtained with other methods (such as gyratory), and was less consistent with the target and in-field reference values. Hartman et al. [44] stated that the Marshall compactor did not have a kneading action to readjust the particle size distribution and therefore, produced a lower density than the values obtained in the field.

The moulds used in this compaction were not the most suitable for cold mixes, as they also do not have any holes to let water flow out, as was the case of the moulds in the gyratory compaction. Furthermore, impact compaction is an especially aggressive type of compaction, which frequently leads to a deterioration of the specimens. Thus, this compaction method is again not recommended for CIR-type mixtures.

Gyratory compaction was generally chosen as the laboratory compaction method best suited to obtain a more homogeneous and uniform compaction and air void distribution [43,46], and the engineering properties were more consistent with those obtained in the field cores. Gyratory compaction was also seen to simulate the conditions of field compaction by the effect of the kneading movement. It allowed better control of the compaction than other methods, and was able to monitor the change in the height of the specimen through the compaction curve.

Once the gyratory compaction method has been chosen as the most suitable, the procedures for calculating the volumetric properties need to be discussed. Regarding the bulk density procedures carried out, it could be concluded beforehand that because of the mentioned porosity of the CIR, the "sealed specimen" procedure

was the most appropriate method to analyse the compaction of these mixtures. According to this bulk density procedure, it was found that 120 compactor gyrations were adequate to reach the target density, thus confirming that the compaction indicated in the Spanish PG-4 [17] was consistent. However, the dimension's procedure yielded quite similar results (differences in the density values were approximately 0.80% in the range of the design gyrations), reaching the target density in 140 gyrations. This procedure was simpler than the prior procedure and allowed the specimens to be reused after the density calculation. Thus, the dimension's procedure could also be used to obtain the bulk density of CIR for laboratory design.

Regarding the real in-field performance, it was observed that the volumetric results obtained following the dry procedure were more in accordance with data from real in-field studies and reports, in terms of densities and air void content, for the lower rotation cases, as expected from the literature. Given the variability of the CIR, it is always interesting and advisable to carry out a test section to really understand how the mixture would behave, once it is executed in the field, and then evaluate its correct curing.

6. Conclusions

In this study, the effects of three different laboratory compaction procedures (gyratory, static, and Marshall) on the volumetric performance of CIR were investigated. Specimens with the same mixture proportions were manufactured by varying the parameters of the compaction methods (i.e., number of gyrations and number of blows), and the volumetric properties were evaluated by different methods, namely bulk density by dimensions, sealed specimen and dry procedures, in addition to the air void content. The results were compared with one another with the design target value, and with the reference range of in-field densities; the most suitable compaction method for CIR mixtures was identified.

As a result, the following conclusions and recommendations were drawn:

a) The density values before curing ($\rho_{o,g}$) were always higher than those after curing obtained by dimensions and sealed specimen procedures ($\rho_{b,g}$ or $\rho_{b,s}$) owing to water filling in the pores before being evaporated. $\rho_{o,g}$ was, on an average, 2.20% higher than $\rho_{b,g}$, with an almost constant offset for all the gyration cases. Bulk density results obtained by the sealed specimen procedure ($\rho_{b,s}$) resulted in a value, which was, on an average, 1.50% higher than that obtained by the dimensions procedure ($\rho_{b,g}$).

b) The bulk density results obtained by the dry procedure ($\rho_{b,d}$) values were significantly higher than those obtained using the other two methods. $\rho_{b,d}$ was 13.18% higher, on average, than $\rho_{b,s}$, and 14.31% higher than $\rho_{b,g}$.

c) Gyratory compaction is the procedure that best fits the target bulk density suggested in the specification referred to, which was reached after 120 gyrations for $\rho_{b,s}$, and after 140 gyrations for $\rho_{b,g}$. Concerning the in-field reference compaction, it was found that $\rho_{b,d}$ gave more realistic results, more similar to the usual average in-field densities and air void content. These in-field approximations were already associated with the lowest cases of gyrations (50 to 100 gyrations), which was in line with results from other CIR studies.

d) By calculating the difference in the weight of the specimens before and after the curing, the water losses owing to evaporation could be estimated. The difference between this estimation and the theoretical water of the mixtures was only 0.94%., and it was concluded that the manufacturing and curing procedures were carried out correctly.

e) Because the inner diameter of the mould was used for the calculation of $\rho_{o,g}$, instead of the actual diameter of the specimens, this density results from the compactor calculations, prior to the curing procedure, were under-predicted by approximately 0.50%. However, this was a small error, and this density calculation is still considered a useful tool, as it is very simple and allows an easy monitoring of the compaction process.

f) A static compaction of 21 MPa returned excessive bulk density results ($\rho_{b,s}$ and $\rho_{b,s}$). In contrast to the gyratory cases, the static case always exceeded the target density significantly, yielding results that are more similar to those obtained from the dry procedure ($\rho_{b,d}$) in the gyratory cases. These high-density results were typically caused by the higher pressure applied to the specimens, aggregate breakage and binder squeezing, and use of unsuitable moulds for cold mixes. Therefore, static compaction was not considered to be the most suitable for CIR mixtures.

g) The bulk densities achieved with the impact-compacted specimens were very low. Neither the in-field reference nor the target density values were achieved. The bulk density of the M−50 group was even lower than that of the G-50 group, and the bulk density of M−75 was similar to that of G-60 or G-70. It was concluded that Marshall compaction was not suitable for CIR mixtures, and resulted in a significant worsening of the volumetric performance. This was possibly a result of the breakage of aggregates during compaction, and the use of an inadequate mould for cold mixtures.

In summary, by looking at the volumetric properties obtained from the three different laboratory compaction methods studied, one can say that the gyratory compactor system turned out to be the most suitable compaction test method for the production of CIR specimens and characterisation in the laboratory; it is also the most comfortable and versatile, and allows to monitor the compaction process during its execution. Regarding the evaluation of volumetric properties, both the bulk density procedures by dimensions and sealed specimen gave very similar results, reaching the target density for the same range of gyrations. However, it was the dry method that yielded results that were more consistent with those achieved in the field.

Author contributions

All the authors, P.O., A.R.P. and I.P. designed the laboratory study, analysed the data and wrote and revised the article.

P.O. performed most of the in-laboratory work, under the guidance of A.R.P. and I.P.

Declaration of Competing Interest

The authors declare that they have no known competing financial interests or personal relationships that could have appeared to influence the work reported in this paper.

Acknowledgements

The authors would like to acknowledge the funding for the project BIA2016-80317-R from the Spanish Ministry of Science and Innovation, with an associated pre-doctoral scholarship for the training of research workers (FPI) BES-2017-079633. The authors would also like to express their sincere gratitude to ARIAS INFRAESTRUCTURAS, and CEPSA and ECOASFALT for their generous donation of RAP and bitumen emulsions, respectively for the pre-

sent research. Finally, an acknowledgement to the Universidade da Coruña/CISUG for funding Elsevier's open access charge.

References

[1] A. Pakes, T. Edil, M. Sanger, R. Olley, T. Klink, Environmental Benefits of Cold-in-Place Recycling, Transp. Res. Rec. 2672 (24) (2018) 11–19, https://doi.org/10.1177/0361198118758691.

[2] A. Kuleshov, Comparative analysis of pavement reconstruction methods, Architect. Eng. 3 (1) (2018) 21–28.

[3] I. Pérez, L. Medina, M.Á. del Val, Mechanical properties and behaviour of in situ materials which are stabilised with bitumen emulsion, Road Mater. Pavement Design 14 (2) (2013) 221–238, https://doi.org/10.1080/14680629.2013.779301.

[4] M.A. Lyubarskaya, V.S. Merkusheva, P.A. Osian, A.A. Ilin, E.S. Svintsov, Integrated approach to using technology of reclaimed asphalt pavement (RAP), Procedia Eng. 189 (2017) 860–866, https://doi.org/10.1016/j.proeng.2017.05.134.

[5] Ministry of Development (2001) "Pavement recycling". Circular Order 8/2001. In Spanish.

[6] F. Xiao, S. Yao, J. Wang, X. Li, S. Amirkhanian, A literature review on cold recycling technology of asphalt pavement, Constr. Build. Mater. 180 (2018) 579–604, https://doi.org/10.1016/j.conbuildmat.2018.06.006.

[7] S. Raschia, C. Mignini, A. Graziani, A. Carter, D. Perraton, M. Vaillancourt, Effect of gradation on volumetric and mechanical properties of cold recycled mixtures (CRM), Road Mater. Pavement Design 20 (sup2) (2019) S740–S754, https://doi.org/10.1080/14680629.2019.1633754.

[8] S. Dessouky, A. Pothuganti, L.F. Walubita, D. Rand, Laboratory evaluation of the workability and compactability of asphaltic materials prior to road construction, J. Mater. Civ. Eng. 25 (6) (2013) 810–818, https://doi.org/10.1061/(ASCE)MT.1943-5533.0000551.

[9] J. Valentin, Z. Čížková, J. Suda, F. Batista, K. Mollenhauer, D. Simnofske, Stiffness characterization of cold recycled mixtures, Transp. Res. Procedia 14 (2016) 758–767, https://doi.org/10.1016/j.trpro.2016.05.065.

[10] P. Liu, H. Xu, D. Wang, C. Wang, C. Schulze, M. Oeser, Comparison of mechanical responses of asphalt mixtures manufactured by different compaction methods, Constr. Build. Mater. 162 (2018) 765–780, https://doi.org/10.1016/j.conbuildmat.2017.12.082.

[11] G.D. Airey, A.C. Collop, Mechanical and structural assessment of laboratory- and field-compacted asphalt mixtures, Int. J. Pavement Eng. 17 (1) (2016) 50–63, https://doi.org/10.1080/10298436.2014.925551.

[12] A. Grilli, A. Graziani, E. Bocci, M. Bocci, Volumetric properties and influence of water content on the compactability of cold recycled mixtures, Mater. Struct. 49 (10) (2016) 4349–4362, https://doi.org/10.1617/s11527-016-0792-x.

[13] J. Marcobal, J. Lizárraga, J. Gallego, Laboratory compaction study and mechanical performance assessment of half-warm mix recycled asphalt mixtures containing 100% RAP, Materials 12 (12) (2019) 1992, https://doi.org/10.3390/ma12121992.

[14] A.H. Martínez, R. Miró, F. Pérez-Jiménez, Spanish experience with gyratory compactor and indirect tensile test in design and control of cold recycled asphalt pavement, Transp. Res. Rec. 2001 (1) (2007) 163–168, https://doi.org/10.3141/2001-18.

[15] G. Tebaldi, E.V. Dave, P. Marsac, P. Muraya, M. Hugener, M. Pasetto, A. Graziani, A. Grilli, M. Bocci, A. Marradi, L. Wendling, V. Gaudefroy, K. Jenkins, A. Loizos, F. Canestrari, Synthesis of standards and procedures for specimen preparation and in-field evaluation of cold-recycled asphalt mixtures, Road Mater. Pavement Design 15 (2) (2014) 272–299, https://doi.org/10.1080/14680629.2013.866707.

[16] Cox, B. C., & Howard, I. L. (2015). Cold in-place recycling characterization framework and design guidance for single or multiple component binder systems (No. FHWA/MS-DOT-RD-15-250-Volume 2).

[17] Ministry of Development (2017) Recycling of bituminous pavements and roadways. Circular Order 40/2017. In Spanish.

[18] P. Orosa, A.R. Pasandín, I. Pérez, Assessment of two laboratory design methods for CIR mixtures with bitumen emulsion based on static and gyratory compaction, Constr. Build. Mater. 265 (2020) 120667, https://doi.org/10.1016/j.conbuildmat.2020.120667.

[19] B.K. Diefenderfer, A.K. Apeagyei, A.A. Gallo, L.E. Dougald, C.B. Weaver, In-place pavement recycling on I-81 in Virginia, Transp. Res. Rec. 2306 (1) (2012) 21–27, https://doi.org/10.3141/2306-03.

[20] Lee, K. W., Brayton, T. E., & Harrington, J. (2003, January). New mix-design procedure of cold in-place recycling for pavement rehabilitation. In Proceedings of the 82nd TRB Annual Meeting.

[21] Sufian, Z., Matori, M. Y., & Hussain, M. Z. (2008). Mix design for cold-in-place pavement recycling; does it guarantee performance? In PROCEEDINGS OF THE 3RD EUROPEAN PAVEMENT & ASSET MANAGEMENT CONFERENCE (EPAM3) 7-9 JULY 2008, COIMBRA, PORTUGAL.

[22] S.A. Cross, Determination of Ndesign for CIR mixtures using the Superpave gyratory compactor, University of Kansas Center for Research, Incorporated, 2002.

[23] M.J. Martínez-Echevarría, R.M. Recasens, M.D.C.R. Gámez, A.M. Ondina, In-laboratory compaction procedure for cold recycled mixes with bituminous emulsions, Constr. Build. Mater. 36 (2012) 918–924, https://doi.org/10.1016/j.conbuildmat.2012.06.040.

[24] R. Miro, Evaluación de los métodos de reciclado y rehabilitación de firmes a partir del análisis de los tramos experimentales del proyecto europeo PARAMIX, Infraestructura Vial 110 (18) (2007). In Spanish.

[25] Piratheepan, M. (2011). Designing Cold Mix Asphalt (CMA) and Cold-In-Place Recycling (CIR) Using Superpave Gyratory Compactor (Doctoral dissertation).

[26] Flores Cuevas, G. A. (2019). Optimization of cold mixtures with emulsion and high rap content (Doctoral dissertation, Universidad Politécnica de Madrid).

[27] S. Thapa, Design of Cold-In-Place Recycling (CIR) Using Superpave Gyratory Compactor, University of Nevada, Reno, 2015.

[28] A. Chomicz-Kowalska, P. Ramiączek, Comparative evaluation and modification of laboratory compaction methods of road base mixtures manufactured in low-emission CIR technology with foamed bitumen and bitumen emulsion, Procedia Eng. 172 (2017) 560–569, https://doi.org/10.1016/j.proeng.2017.02.066.

[29] AENOR, Spanish Association for Standardisation and Certification, 2015. UNE-EN 12697–2. Bituminous mixtures. Test methods. Part 2: Determination of particle size distribution. Madrid, Spain. In Spanish.

[30] AENOR, Spanish Association for Standardisation and Certification, 2006. UNE-EN 1097-6. Tests to determine the mechanical and physical properties of aggregates. Part 6: Determination of particle density and water absorption. Madrid, Spain. In Spanish.

[31] Ministry of Public Works and Transport, 1990. NLT standards. NLT-164/90. Binder content in bituminous mixtures. Road tests. Directorate General for Roads, 2nd ed. Madrid, Spain. In Spanish.

[32] AENOR, Spanish Association for Standardisation and Certification, 2015. UNE-EN 1426. Bitumen and bituminous binders. Determination of needle penetration. Madrid, Spain. In Spanish.

[33] AENOR, Spanish Association for Standardisation and Certification, 2015. UNE-EN 1427. Bitumen and bituminous binders. Determination of the softening point. Ring and Ball method. Madrid, Spain. In Spanish.

[34] AENOR, Spanish Association for Standardisation and Certification, 2013. UNE-EN 13808. Bitumen and bituminous binders. Framework for specifying cationic bituminous emulsions. Madrid, Spain. In Spanish

[35] AENOR, Spanish Association for Standardisation and Certification, 2012. EN 12697-6. Bituminous mixtures. Test methods for hot bituminous mixtures. Part 6: Determination of apparent density of bituminous samples. Madrid. In Spanish

[36] AENOR, Spanish Association for Standardization and Certification, 1994. UNE-EN 103-501-94. Geotechnics. Compaction test. Modified Proctor. Madrid. In Spanish

[37] Ministry of Public Works and Transport, 2002. NLT standards. NLT-162. Effect of water on the cohesion of compacted bituminous mixtures (Immersion-compression test). Road tests. Directorate General for Roads, 2nd ed. Madrid, Spain. In Spanish

[38] AENOR, Spanish Association for Standardization and Certification, 2008. UNE-EN 12697-31. Bituminous mixtures. Test methods for hot bituminous mixtures. Part 31: Specimen preparation by gyratory compactor. Madrid. In Spanish

[39] Ministry of Public Works and Transport, 2002. NLT standards. NLT-161. Compressive strength of bituminous mixtures. Road test. Madrid, Spain: Center for the Study and Experimentation of Public Works (CEDEX); 2002. In Spanish

[40] AENOR, Spanish Association for Standardization and Certification, 2013. UNE-EN 12697-30. Bituminous mixtures. Test methods for hot bituminous mixtures. Part 30: Specimen preparation by impact compactor. Madrid. In Spanish

[41] AENOR, Spanish Association for Standardisation and Certification, 2010. EN 12697-5. Bituminous mixtures. Test methods for hot bituminous mixtures. Part 5: Determination of the maximum density. Madrid. In Spanish

[42] AENOR, Spanish Association for Standardisation and Certification, 2020. EN 12697-8. Bituminous mixtures. Test methods. Part 8: Determination of voids content of bituminous specimens. Madrid. In Spanish

[43] D. Lo Presti, R. Khan, N. Abdul Hassan, G. Airey, A. Collop, Laboratory mix design of asphalt mixture containing reclaimed material, Adv. Mater. Sci. Eng. 2014 (2014), https://doi.org/10.1155/2014/507082.

[44] A.M. Hartman, M.D. Gilchrist, G. Walsh, Effect of mixture compaction on indirect tensile stiffness and fatigue, J. Transp. Eng. 127 (5) (2001) 370–378, https://doi.org/10.1061/(ASCE)0733-947X(2001)127:5(370).

[45] Bonnot, J. (1997). Selection and use of the procedures for laboratory compaction of bituminous mixtures. In PERFORMANCE RELATED TEST PROCEDURES FOR BITUMINOUS MIXTURES. PROCEEDINGS OF THE WORKSHOP HELD DUBLIN 6-7 NOVEMBER 1997.

[46] L. Gao, F. Ni, H. Luo, S. Charmot, Characterization of air voids in cold in-place recycling mixtures using X-ray computed tomography, Constr. Build. Mater. 84 (2015) 429–436, https://doi.org/10.1016/j.conbuildmat.2015.03.081.

[47] J. Lin, L. Huo, F. Xu, Y. Xiao, J. Hong, Development of microstructure and early-stage strength for 100% cold recycled asphalt mixture treated with emulsion and cement, Constr. Build. Mater. 189 (2018) 924–933, https://doi.org/10.1016/j.conbuildmat.2018.09.064.